The autocorrelation function of the north pole dust

Jens Knude
Copenhagen University Observatory
Copenhagen, Denmark

N91-14901

1. Abstract

The angular scales on which local interstellar dust is distributed are so far rather unknown as are the geometrical shapes of the dust features.

From the about 5000 color excesses resulting from a north polar survey with 4-5 stars per square degree the two-point autocorrelation function is derived for separations ranging from 10 ' to 3 °.

For intercloud lines of sight, -0.020 < E(b-y) < -0.010 mag, the average cross products $\langle E_1 \times E_2 \rangle_\Theta$ show no variation with separation Θ(1,2) whereas products of cloud column densities, 0.030 < E(b-y) < 0.040 mag, seem to prefer discrete separations either less than 20', around 75' or finally at about 150'.

Surprisingly the two point autocorrelation function $\omega_E = \langle E_1 \times E_2 \rangle / \langle E \rangle^2 - 1$ equals 0 except for any separation except Θ=0. $\omega_E(\Theta)$'s absence of variation is unexpected because $\omega_H(\Theta)$ is known to vary exponentially above b = 40° for separations less than 3 °. Atomic hydrogen and dust may thus not be entirely mixed or the moments $\langle E_1 \times E_2 \rangle_\Theta$ may not characterize the dust distribution.

2. Angular distribution of almost identical reddening pairs.

Apparently the north polar cap is not completely free from interstellar dust. Figure 1 gives an empression of the dust column densities which may be expected for b > 40° and within ≈ 500 pc from the plane. $A_V = \frac{1}{10}$ corresponds to E(b-y) ≈ 0.024 mag so a substantial fraction of the observed lines of sight, almost one third in fact , is fairly reddened.

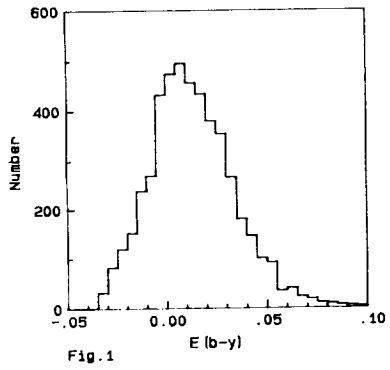

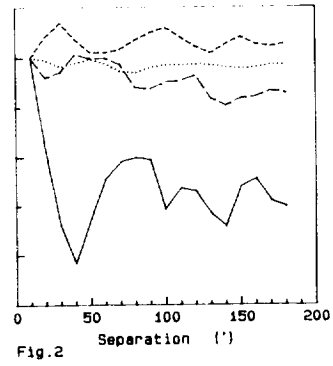

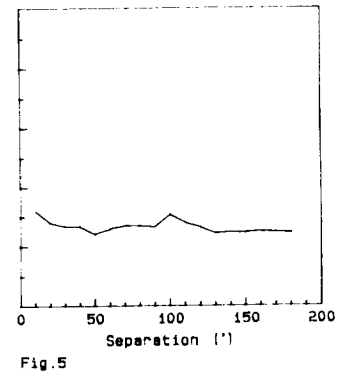

Figure 1. E(b-y) histogram resulting from a survey of the polar area above b=70°. The survey is magnitude compelete for the A5 to G0

stars. The surface density is 4.5 stars per square degree.

Figure 2. Relative frequency of pairs with almost identical color excess: E_2-E_1 = 0.010 mag , as a function of separation. The ordinate is on an arbitrary scale , and the curves are shifted to a common frequency at the 10' separation. The dotted curve corresponds to pairs: -0.020,-0.010. The short dashes corresponds to pairs: 0.010, 0.020. The long dashes corresponds to pairs: 0.020,0.030. The solid curve are for pairs with : 0.030,0.040.

*Figure 5.*Average cross product $\langle E_1 \times E_2 \rangle_\Theta$ versus separation.

First we consider how the average values of products of almost identical color excesses vary with separation. If the diffuse dust clouds have spherical projections the function $\langle E_1 \times E_2 \rangle_\Theta$ will be a representation of typical sizes at a given distance. Figure 2 shows the results for a selection of reddening pairs. A changing shape of the curve is noted when the reddenings are changed from those typical for the intercloud directions, (E_1,E_2) = (-0.020, -0.010) , to those with (E_1,E_2) = (0.030, 0.040) probably crossing regions with enhanced dust density. It is clear that $\langle -0.020 \times -0.010 \rangle_\Theta$ does not change with separations smaller than 3°. So if we consider an intercloud line of sight it will always be located in a region with an extent of at least 3° - its shape untold. For the slightly obscured lines of sight the average product does vary with separation. With E_1 in the range 0.030± 0.005 and E_2 in the interval 0.040± 0.005 the most probable separation is less than 20' but secondary maxima at 75' and 150' are also suggested.

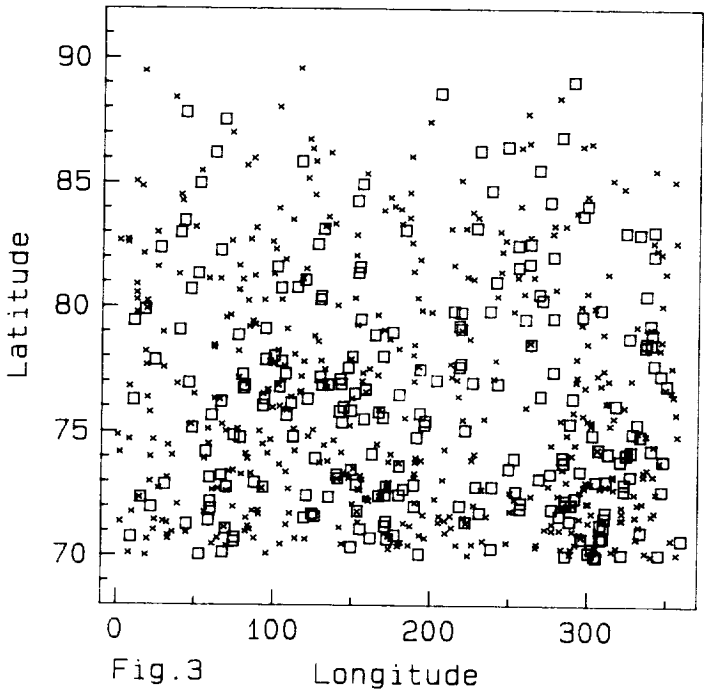

Fig.3

Figure 3. Location of the E_1=0.030± 0.005 (*the* ×*'s*) and the E_2=0.040± 0.005 (□*'s*) lines of sight.

The existence of these preferred separations does, however, not necessarily bear on the angular sizes of discrete clouds. The sequence of preferred separations does not indicate that there are unique upper limits to cloud diameters but more likely it suggests that the dust may not entirely be localized in spherical structures but that it just as well could be confined to elongated features. This qualitative interpretation of Figure 2 may partly find support in Figure 3 where E_1 = 0.030 (*the* ×'*s*) and E_2 = 0.040 (□'*s*) lines of sight are indicated in a (l,b) diagram. What Figure 3 show are several examples where E_1 and E_2 are confined to string-like features. Figure 3 is furthermore instructive by displaying the very inhomogenous distribution of the cloud lines of sight E_1,E_2 and particularly by showing the existence of large solid angles void of these clouds, e.g. the regions centered on (l,b) = (250,75) and (50,79).

3. An overall view of obscured lines of sight.

On Figure 4 is shown the (l,b) distribution of all lines of sight with E(b-y)$\gtrsim$ 0.024 mag on two different scales and in a polar representation. The different scales are chosen to aid the eye to see various structures. The justification of the lower redddening limit 0.024 mag is threefold.

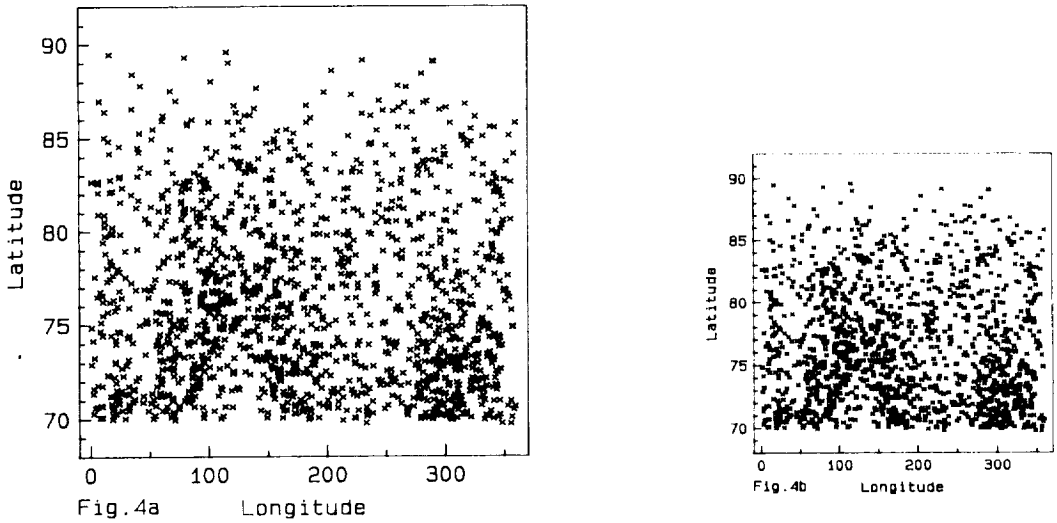

Figure 4a and b. Lines of sight with E(b-y) > 0.024 mag shown in (l,b)-diagrams with different resolution. There is apparently some structure in the distribution of the larger color excesses.

First the lower limit corresponds to $3\times\sigma(E(b\text{-}y))$ so there is a high probability that the plotted lines of sight are significantly reddened. Second , E(b-y) = 0.024 is the reddening expected in the most typical cloud from a decomposition of the color excess distribution in the galactic plane by the method of moments , assuming only one type of clouds. Finally E(b-y) = 0.024 corresponds to $\tau(E{=}250eV)$ = 1 , assuming a canonical gas/dust ratio with no clumping. The E(b-y) > 0.024 mag map may thus indicate where a 250 eV

emission , originating in the more remote halo , could be absorbed. The lower resolution of Figure 4b and 4d suggests the possibility of large more or less coherent systems of extinction at the north galactic pole. Several odd features are also noted in Figure 4a such as the doughnut shaped structure centered at (l,b) = (100,76.5): an isolated ring with $A_V \geq$ 0.1 mag with no absorption at its center. Note also the long string of large excesses at (l,b) = (340-350, 76-84) in an otherwise almost extinction free region.

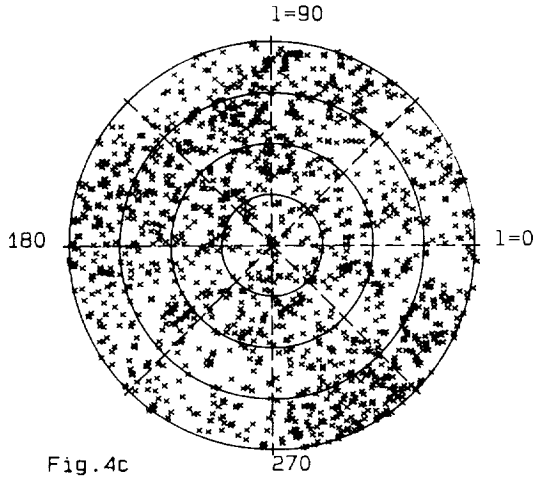

Fig.4c

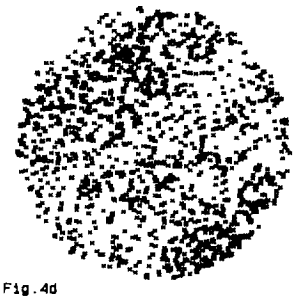
Fig.4d

Figure 4c and d. As Figure 4a and b but in a polar layout. The separation between the latitude circles in Figure 4c is 5°.

Finally Figure 4c,d give the polar presentation of the dust distribution. Particularly the compressed version in which the individual dust features have merged gives an impression of how the dust is located at the NGP.

4. The two-point autocorrelation function.

After the presentation of the complex projected dust distribution in the previous sections it would be interesting to known the behaviour of a statistics as the two point autocorrelation function: $\omega_E(\Theta)=\langle E_1 \times E_2 \rangle / \langle E \rangle^2 - 1$. As the distribution in Figure 4d is not quite unlike the projected distributions of galaxy counts one might perhaps expect a correlation function similar to those of the galaxy distributions. However , the two-point autocorrelation function of the polar dust distribution is surprisingly found to be constantly equal to zero, except for Θ = 0. The projected dust distribution is apparently uncorrelated conversely to the atomic hydrogen whose autocorrelation follows an exponential law for separations smaller than 3° at latitudes above 40 °.

The different correlation functions could be due to a different spatial distribution of gas and dust or be an artefact of the different observing techniques.

5. Conclusion

The data presented may possibly best be understood if the dust mostly is located in inhomogeneous strings or sheets of substantial angular size.